

# Experimental Investigation on Metallurgy of High Vacuum Electron Beam Welded Ni Base Alloy Inconel 718

Jalpa Zalawadia<sup>1</sup> and Kulbhushan Kumar Lamba<sup>2</sup>

Mechanical Engineering Department, Faculty of Engineering and Technology, Parul University, Vadodara, Gujarat, India  
E-mail: <sup>1</sup>jcadroja@gmail.com, <sup>2</sup>kbklamba@yahoo.in



DOI: 10.22486/iwj/2017/v50/i3/158284

## ABSTRACT

The excellent weld quality of Inconel 718, among the class of Ni, Cr precipitation hardenable alloys is well recognised. Electron Beam Welding (EBW) (especially the high vacuum) is the most preferred technique, to impart the optimum level of properties, as is demanded for many of its critical applications in the fields of Nuclear power and Aerospace. This paper examines in detail the microstructure of weldments obtained in different material conditions i.e. with parent material in solution treated condition, in double aged condition and the ones weld in solution treated condition and administered varied post weld heat treatments, along with compositional analysis i.e. EDAX, and the effect of weld heat on grain structure. This paper also highlights and contrasts evaluation of weld properties of Inconel 718 by Electron Beam Welding in comparison with laser beam welding (LBW).

**Keywords:** Microstructure; composition analysis; weld heat; grain morphology; grain boundary segregation.

## 1.0 INTRODUCTION

Inconel 718 is a Ni-Cr precipitation hardenable alloy containing higher amount of iron, niobium and molybdenum and lesser amounts of aluminum and titanium. The alloy has corrosion resistance and high temperature strength with outstanding weldability and resistance to post weld heat cracking [1]. Inconel 718 has excellent creep-rupture strength at temperature up to 700°C (1300°F). It is used as a base material in making of liquid sodium cooled fast breeder reactors, in fabrication of liquid rocket motors, after burner liners and as combustion cans in a wide variety of application. [1]. This superalloy has a Nickel Iron-Chromium matrix and aluminum and titanium which are alloying elements that produce secondary phases such as Ni<sub>3</sub>(Al, Ti) ( $\gamma'$ ) gamma prime; Ni<sub>3</sub>Nb ( $\delta''$ ) gamma double prime, delta ( $\delta$ ) orthorhombic Ni<sub>3</sub>Nb and other topologically close packed phases such as Laves phase. Various heat treatment like double aging help

increase in its structural stability by inducing the precipitation of gamma prime ( $\gamma'$ ) and gamma double prime ( $\gamma''$ ), which offers the mechanical strength of Inconel 718 [2] [3].

As an extension to the earlier research work [4] carried on the subject topic of Electron Beam Welding of Ni base alloy 718, where in extensive experimental investigations were carried out to quantitatively demonstrate the reliability of this process by subjecting the welds to quality evaluation by radiographic examination of welds, joint efficiencies, residual stresses, metallographic examination of welds as well as effect of post weld heat treatment (PWHT) on mechanical properties. This study investigates

- (A) The microstructure of different variants of the welded specimens, i.e. (i) Welded in solution treated condition (as received), (ii) Welded in aged condition (iii) Welded in solution treated condition (as received) and subsequently subjected to double aging treatment.

- (B) SEM/EDAX Analysis of the basic material constituents across the different weld zones i.e. Fusion Zone, Heat Affected Zone and Base Metal for different variants of welded samples as above.
- (C) Examination of various phases formed in Electron Beam Welded Specimens.
- (D) The effect of weld heat on
  - (i) Grain morphology
  - (ii) Microstructure
  - (iii) Mechanical Properties

## 2.0 EXPERIMENTAL PROCEDURE

The experimental procedure i.e. examination of microstructure of the welded specimens was undertaken to demonstrate above stated objectives with the help of Optical microscope with CCD camera attachment (model EPY TYP-II Carl Zeiss, Jena) and EDS analyser (Oxford Instruments S Max 20, 2012).

Aging treatment consisted of the following steps:

- i. 8 hrs at 720°C (1325°F),
- ii. Furnace cool to 620°C (1150°F)
- iii. Hold for 8 hrs at 620°C (1150°F) & then
- iv. Air cool

Solution treatment consisted of the following steps:

- i. Heating to 955°C (1750°F), hold for 1 hour & then
- ii. Air cool

## 3.0 RESULTS AND DISCUSSION

### 3.1 The Microstructure of the Welded Specimens

Microstructural Examination of Electron Beam welded Specimen is detailed below

**Fig. 1** shows Microstructure at parent metal shows fine nickel solid solution grain with twins. Second phase precipitates are observed at the grain boundaries. Microstructure at HAZ shows fine nickel solid solution grain with twins. Second phase precipitates are observed within the grains. Microstructure at weld shows dendritic structure of nickel solid solution with secondary precipitates. Etchant used is Glyce-regia.

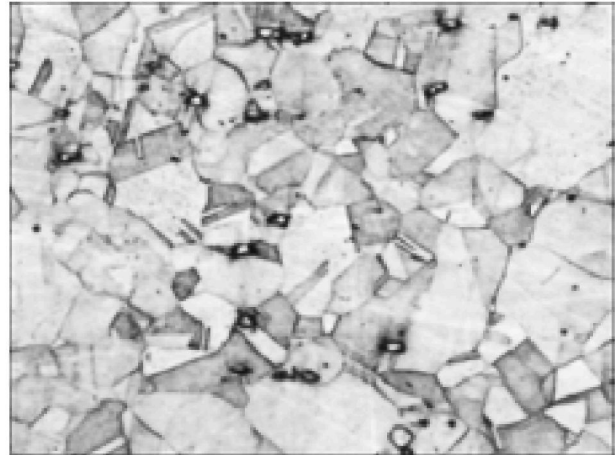


Fig. 1(i)

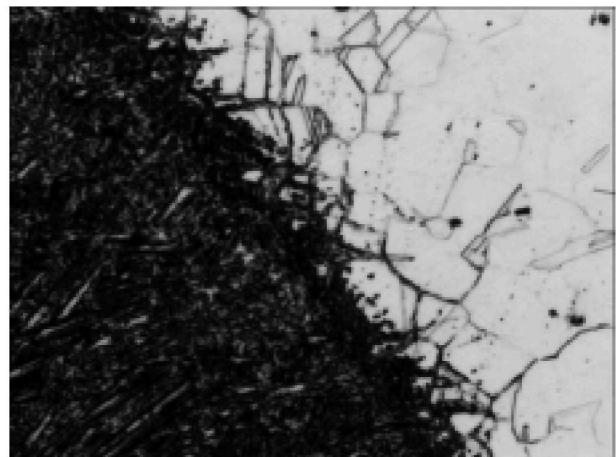


Fig. 1(ii)

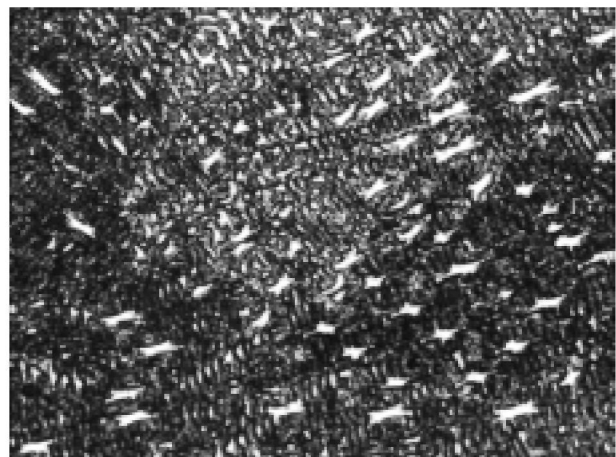


Fig. 1(iii)

**Fig. 1: Electron beam welded specimen with plates (as received) in solution treated condition for (i) Base Metal (ii) HAZ (iii) Fusion Zone at 400X**

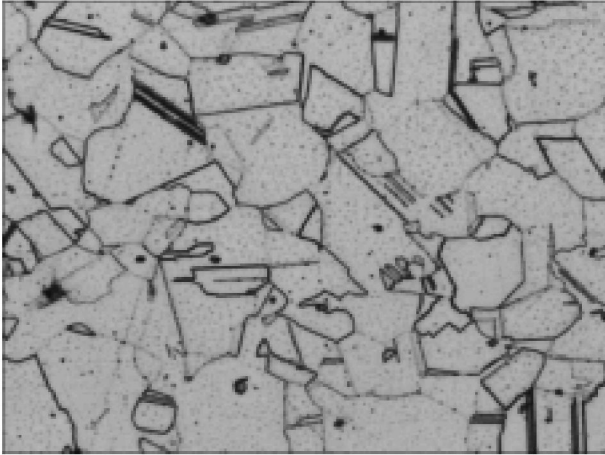


Fig. 2(i)

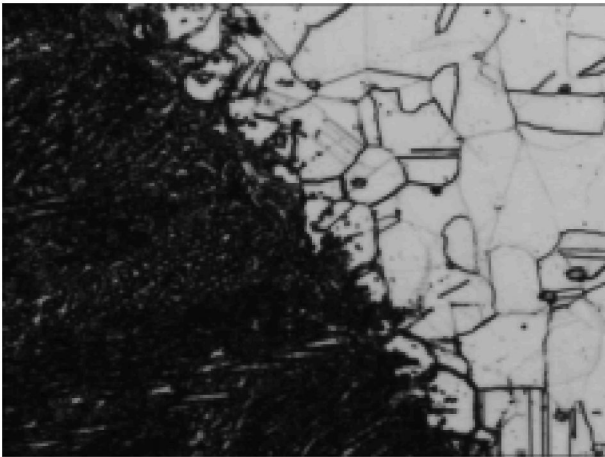


Fig. 2(ii)

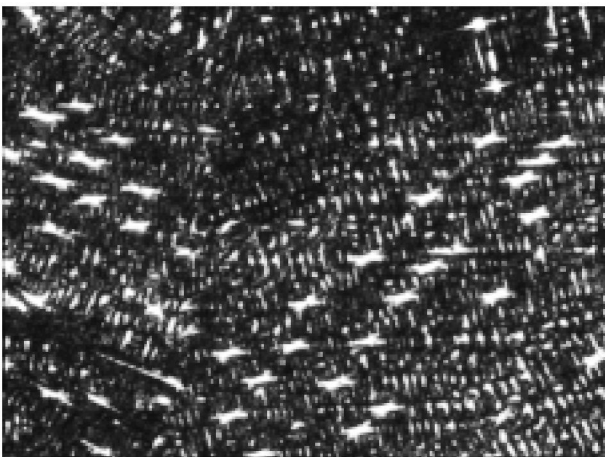


Fig. 2(iii)

**Fig. 2 : Electron beam welded specimen with plates (as received) in aged condition for (i) Base Metal (ii) HAZ (iii) Fusion Zone at 400X**

**Fig. 2** shows Microstructure at parent metal shows fine nickel solid solution grain with twins. Second phase precipitations are observed within the grains.

Microstructure at HAZ shows fine nickel solid solution grain with twins. Second phase precipitations are observed within the grain. Microstructure at weld shows dendritic structure of nickel solid solution with secondary precipitates. Etchant used is Glyce-regia.

**Fig. 3** shows the microstructure of the sample which has given Post Weld Heat Treatment, the coarsening of grains is observed compared with other two samples. Microstructure at parent metal shows coarse nickel solid solution grain with twins. Second phase precipitates are observed within the grain.

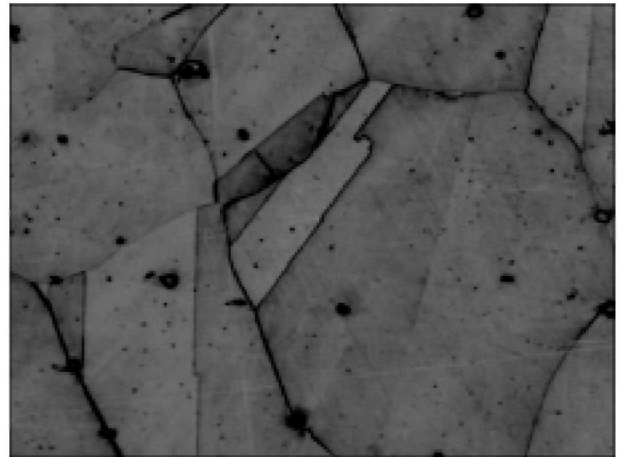


Fig. 3 (i)

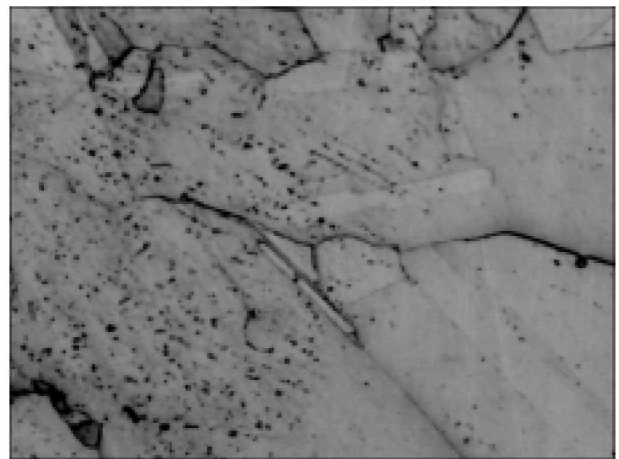
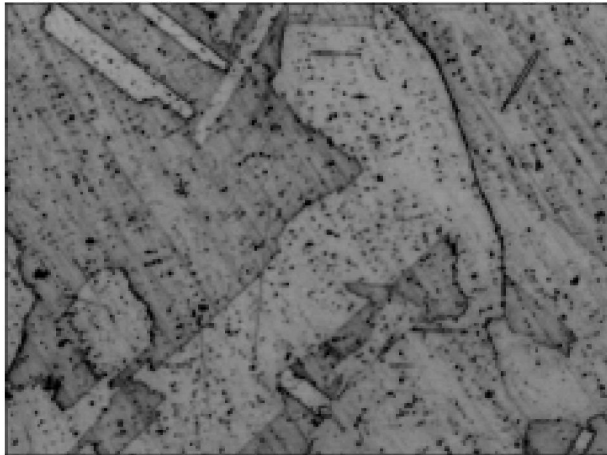


Fig. 3 (ii)



**Fig. 3(iii)**

**Fig. 3 : Electron beam welded specimen with plates welded in solution treated condition (as received) and subsequently given PWHT i.e. solution treatment at 2000 F+ Double aged at 720°C (1325 F) / 620°C (1150 F) for (i) Base Metal (ii) HAZ (iii) Fusion Zone at 400X**

Microstructure at HAZ shows coarse nickel solid solution grain with twins. Second phase precipitates are observed within the grain. Microstructure at weld shows dendritic structure of nickel solid with secondary precipitates. Etchant used is Glyce-regia.

Based on above results microstructure examination of specimens welded with plates as received in solution treated condition and the ones received in aged condition shows fine nickel solid solution grains with twins and the second phase precipitates observed, both in the Base metal and Heat Affected Zone at the grain boundaries which confirms strengthening of the material. No micro fissures were observed in the HAZ. Also the fusion zone was free from micro/ macro cracks.

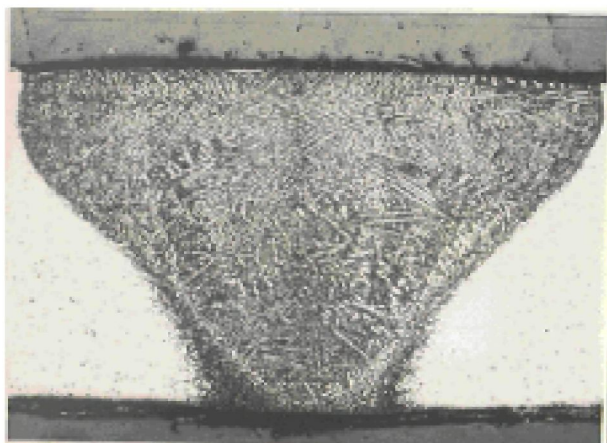


**Fig. 4 : Microstructure of weld bead**

**Fig. 4** indicates the microstructure at weld bead. Examination of weld bead exhibited absence of centerline grain boundary, a potentially harmful defect in a weld. Normally it is the last region of the weld to solidify and is enriched in alloying elements and impurities. Low melting point constituents of a centerline grain boundary are principally responsible for lower mechanical/corrosion resistance, low toughness as compared to other grain boundaries which makes it more susceptible to crack propagation [5].

A dendritic structure was observed in the weld zone. Inter-dendritic region reveals the presence of Laves phase particles and plate-like delta -phase. Microstructure examination of the weld zones reveals presence of a fine dendritic structure as expected. EDAX analysis confirmed presence of 'Laves phase' in Fusion as well as in the Heat Affected Zone See **Fig.4**. Rapid cooling rates and presence of wide alloying elements gives rise to very fine dendritic structure in the fusion zone.

Microstructure of specimens given solution treatment and then welded and subsequently given PWHT i.e. Solution Treatment at 2000 F + Double aged at 720°C (1325 F) / 620°C (1150 F) reveals coarser nickel solid solution grain with twins for Base metal and Heat Affected Zone. Second phase precipitates are also observed within the grains (Refer **Fig.3(i)** and **Fig.3(ii)**). Microstructure at weld shows (Refer **Fig.3(iii)**) dendritic structure of nickel with secondary precipitates. After the post heat treatment slightly coarsened grains were observed in HAZ (**Fig. 3(iii)**).

The solidification of Inconel 718 starts with Primary liquid  $\rightarrow$  gamma reaction results in increase of Nb, Mo, Ti and C in inter-dendritic liquid. Then liquid  $\rightarrow$  (gamma + NbC) eutectic reaction consumes most of carbon available in the alloy until another eutectic type reaction liquid  $\rightarrow$  (gamma + Laves phase) takes place; this reaction terminates the solidification process. Niobium segregation during the process of solidification of the weld zone is basically responsible for the formation of Laves phase [5].

High cooling rates in Electron Beam Welding, in comparison with other conventional welding processes, substantially reduces the niobium segregation and thus reduces formation of detrimental Laves phase and lower niobium concentration in Laves phase because of the insufficient time for solute redistribution [5]. This is in line with observation made by X. Cao et al.

Microstructure examination also showed complete absence of grain boundary segregation of constituent elements and were

found free from micro fissures or grain boundary cracks. Further Microstructure examination reveals absence of liquation cracks, hot/lamellar tearing of welded specimen.

### 3.2 SEM/EDAX Analysis

An extensive EDAX analysis was undertaken on the parent metal, weld zone and HAZ, for the three aforesaid variants of Electron Beam Welded Specimens as detailed below.

#### Plates welded in solution treated condition

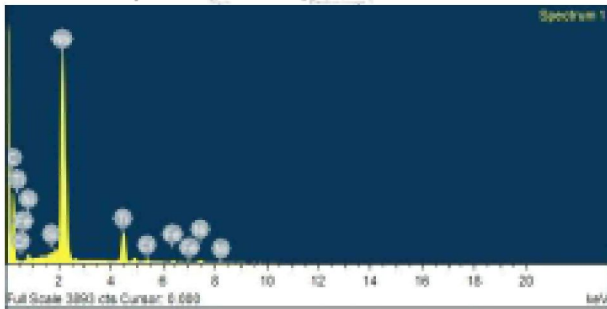
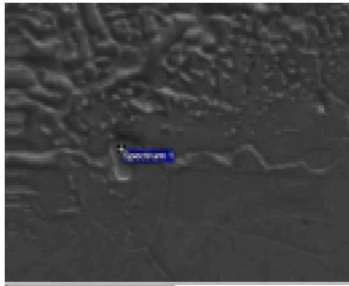


**Fig. 5 : EDAX for Particle at HAZ for plates welded in Solution treated condition**

**Fig. 5** for EDAX analysis on Particle at HAZ shows higher % of C, Ti and Nb with depleted presence of Ni, Cr and Fe. The disc shape particle and compositional analysis confirms the presence of  $\gamma'$  – Ni<sub>3</sub>Nb. The strengthening is basically on account of the presence of lens like disc shaped gamma double prime ( $\gamma''$ ) coherent precipitates, wherein niobium is the key alloying element and responsible for the strengthening in  $\gamma''$  phase [6].

**Fig. 6** for EDAX analysis on matrix of HAZ for plates welded in Solution treated condition shows Higher (Almost alloyed composition) amount of Ni, Cr, Fe and that of Nb. The compositional analysis authenticates presence of gamma double prime and gamma prime. Many investigations have proved that major strengthening phase is gamma double

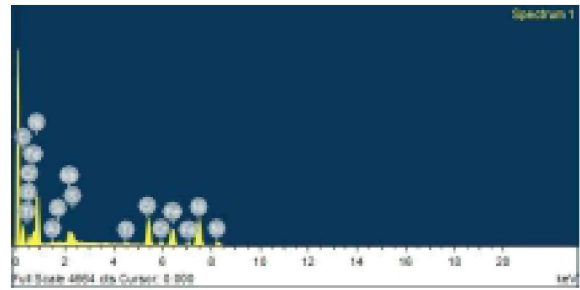
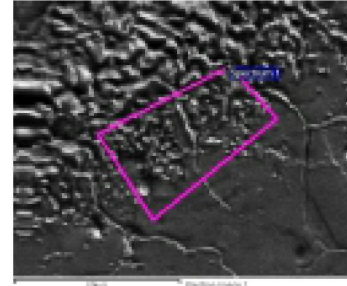


**Fig. 6 : EDAX on matrix of HAZ for plates welded in Solution treated condition**

prime [7]. Presence of this phase on the boundary of fusion/heat affected zone is instrumental in strengthening of the weldment(s). Also Carbon and titanium amount confirms the presence of MC phase, i.e. TiC, Titanium Carbide which appears as globular irregularly shaped particles. Ni<sub>3</sub>Nb observed in overaged IN 718, has an acicular shape when formed between 815°C (1500 F) to 980°C (1800 F).

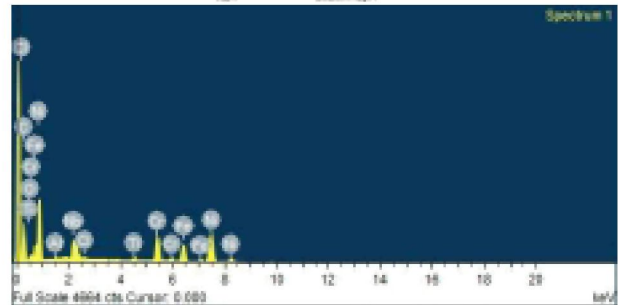
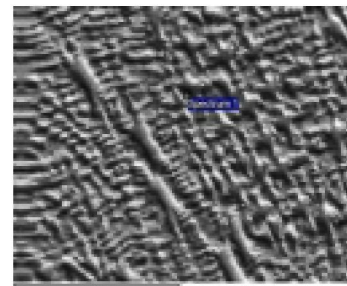


**Fig. 7 : EDAX on Fusion Zone for plates welded in Solution treated condition**

**Fig. 7** depicting EDAX on Fusion Zone for plates after solution treatment and then welding shows the presence of TiC and NbC, which is MC type of carbide. It appears as globular, irregularly shaped particles that are grey to lavender.

**Table-1 : Chemical composition of samples welded in solution treated condition**

	Particle on HAZ	Matrix on HAZ	Particle on PM
Ni	2.73	47.77	45.60
Cr	1.08	16.55	14.75
Fe	1.19	17.18	15.17
Co	-	-	-
Mo	-	-	-
Nb	57.73	5.88	7.36
Ti	9.96	0.86	1.28
Al	-	0.39	0.69
C	27.04	8.87	13.96
Mn	-	-	-
Si	0.28	0.42	-
B	-	-	-
Others	-	1.24O 0.83S	0.640 0.55 Cl

It confirms from the compositional analysis of solution treated samples from **Table 1** that there is no impurity (like Sulphur, boron) on the particle as well as matrix. Segregation of sulphur and boron at the grain boundary is responsible for HAZ cracking and liquation cracking respectively in Inconel 718 [8] [9]. Thus the solution treated and welded samples are free from HAZ cracking and liquation cracking.

**Fig. 8** shows EDAX analysis on Particle at HAZ for plates in Aged condition. This EDAX shows remarkable strengthening of C, Nb & Ti and considerable depletion of Cr, Fe & Ni, which agrees with the fact that various phases are, formed as below.

Gamma double prime (Ni<sub>3</sub>Nb), which is principle strengthening phase in Inconel 718, gamma double prime are coherent disk shaped particles. Furthermore M<sub>23</sub>C<sub>6</sub> {(Cr, Fe)<sub>23</sub>C<sub>6</sub>} is also present. This phase can precipitate as films, globules, platelets, lamellae and cells. It usually forms at grain boundaries. Also MC (TiC, NbC) type of carbide is present, which is confirmed by compositional analysis. It appears as globular, irregularly shaped particles that are grey to lavender.

**Plates welded in Aged condition**

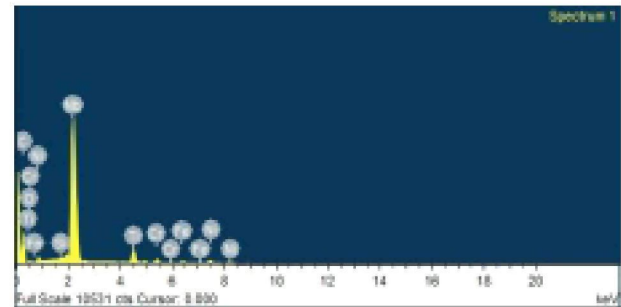
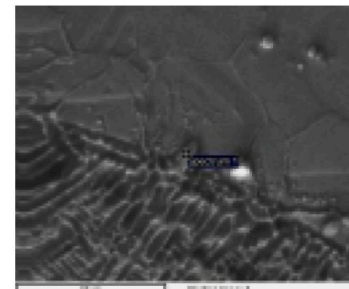


**Fig. 8 : EDAX analysis on Particle at HAZ for plates in Aged condition**

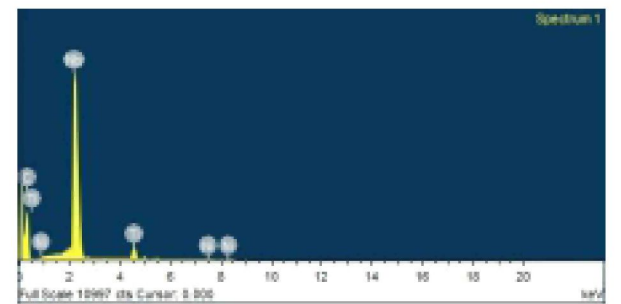
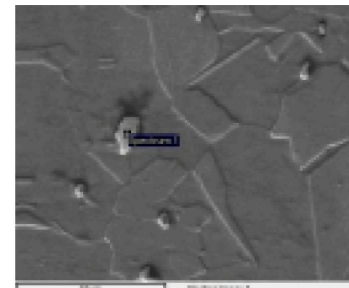


**Fig. 9 : EDAX analysis on particle at Parent Metal for plates in Aged condition**

**Fig. 9** shows EDAX on particle, for both the locations. EDAX was done on a particle, which is MC type delta phase rich in Niobium and Carbon.

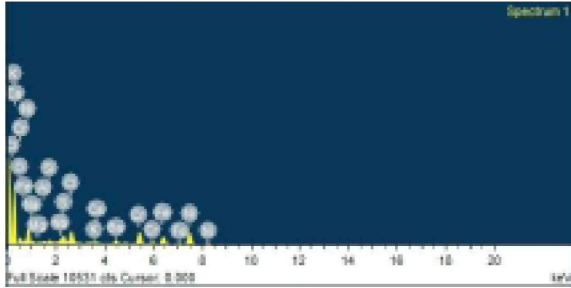
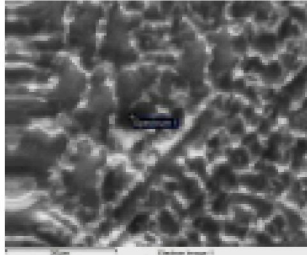


**Fig. 10 : EDAX analysis on Weld for plates in Aged condition**

**Fig. 10** shows EDAX analysis on Weld for plates in Aged condition. By micro structure examination, it shows the laves phase, wherein silicon content also confirms the presence of laves phase. Increased silicon consequently gives greater volume fraction and noticeable rise in stability of laves phase present in the microstructure [10].

**Plates welded and given Post weld Heat Treatment**

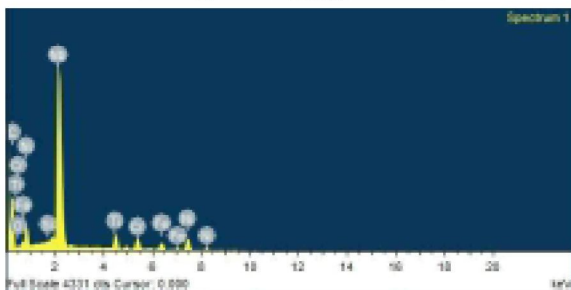
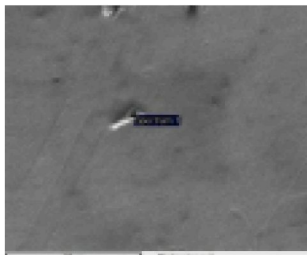


**Fig. 11 : EDAX on HAZ for solution treated and given PWHT**

**Fig. 11** shows EDAX on HAZ for solution treated and given PWHT, which indicates the marked phase shows the Laves + Gamma eutectic in the fusion zone.

**Table -2 : Chemical compositions of samples welded in aged condition**

	Particle on HAZ	Matrix on PM	Particle on Weld
Ni	5.75	1.22	41.42
Cr	2.31	-	16.25
Fe	2.12	-	16.58
Co	-	-	-
Mo	-	-	-
Nb	61.32	66.75	3.61
Ti	6.63	5.17	-
Al	-	-	0.79
C	19.87	26.86	-
Mn	-	-	-
Si	0.36	-	1.29
B	-	-	-
S	-	-	2.62
Other	1.630		1.570 2.62S 1.8 Na 6.07 0.71K 0.25Ca 16.25Cl 6.43Ba

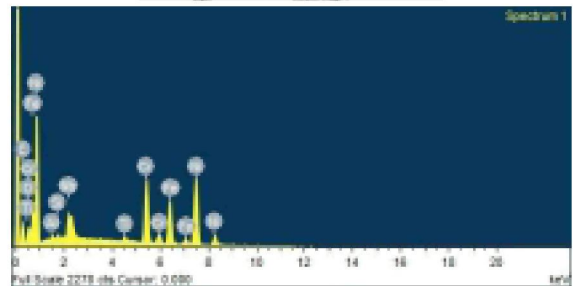
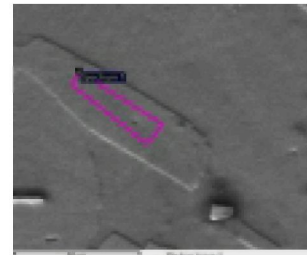


**Fig. 12 : EDAX analysis on particle for solution treated and given PWHT**

**Fig. 12** shows EDAX analysis on particle for solution treated and given PWHT which reveals Nb rich secondary phase (gamma double prime) to be the principle strengthening phase in Inconel 718. The other alloying elements are present relatively in lesser amount with respect to the nominal constitution of the base metal.

The formation of detrimental Laves phase is strongly influenced by solidification conditions. The constituents of Laves particles are usually rich in Nb, Ti, Mo, Si, and lean in Fe, Cr, and Ni with respect to those present in base metal [5]. Moreover the amount of Laves phase and niobium segregation in the weld is determined by the solidification conditions.

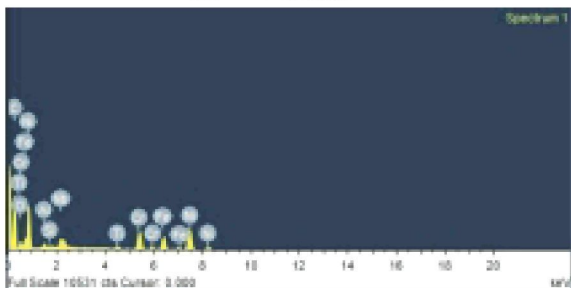
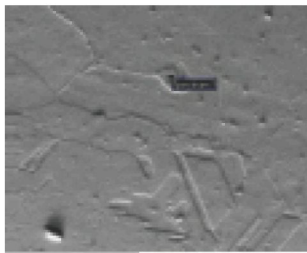


Fig. 13 : EDAX analysis on particle for solution treated and given PWHT

Table 3 : Chemical compositions of samples welded and given Post Weld Heat Treatment

	Particle on BM	Matrix on HAZ	Particle on BM
Ni	12.26	52.31	42.47
Cr	4.29	17.76	13.59
Fe	4.57	18.39	14.76
Co	-	-	-
Mo	-	-	-
Nb	52.75	4.64	3.91
Ti	4.54	0.96	1.08
Al	-	0.39	1.08
C	20.64	4.37	21.31
Mn	-	-	-
Si	0.31	0.40	0.39
B	-	-	-
Other	0.540	0.770	1.60

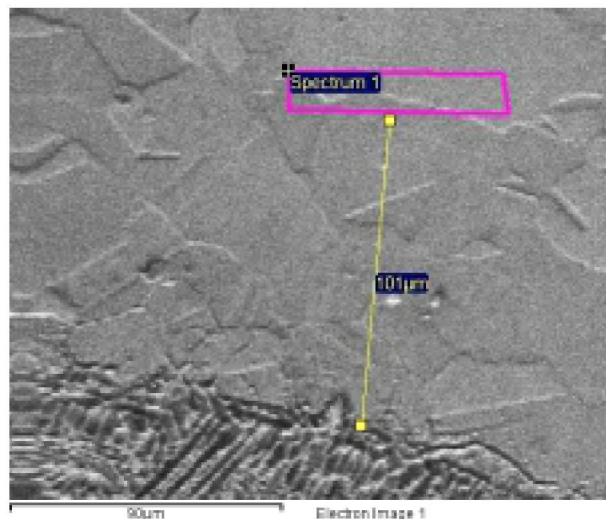


Fig. 14 : SEM image of Aged and welded sample showing Microstructure of HAZ with Laves phase

Table 4 : Chemical composition of Aged sample showing Laves Phase

Elements	Wt. (%)
Titanium	1.71
Chromium	20.28
Iron	19.72
Nickel	58.29

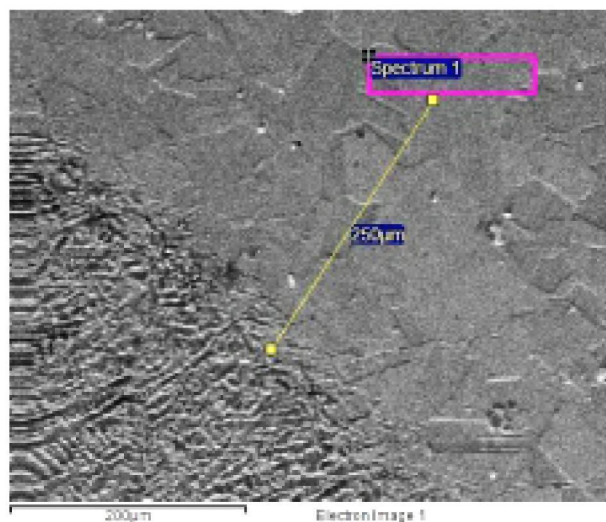
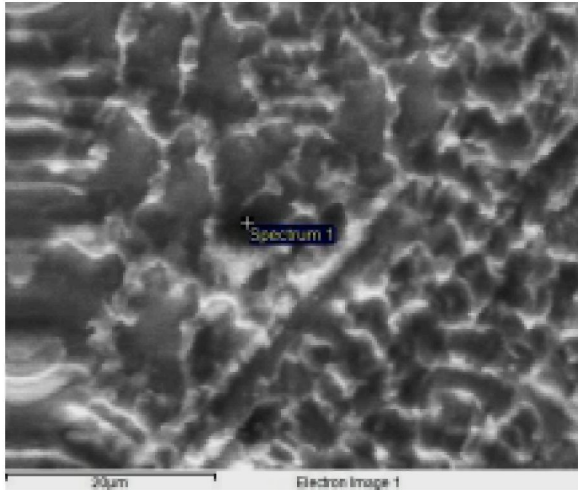


Fig. 15 : SEM image of Aged and welded sample showing Microstructure of HAZ with Laves phase

**Table 5 : Chemical Composition of aged and welded sample of HAZ with Laves Phase**

Elements	Wt. (%)
Chromium	18.08
Iron	25.64
Nickel	56.29



**Fig. 16 : SEM image of Aged and welded sample showing microstructure of Fusion Zone with Laves phase**

**Table 6 : Chemical composition of Aged and welded sample showing microstructure of Fusion Zone with Laves phase**

Elements	Wt. (%)
Aluminium	0.79
Silicon	1.29
Sulfur	2.62
Chromium	16.25
Iron	16.58
Nickel	41.42
Niobium	3.61
Oxygen	1.57
Sodium	1.80
Magnesium	0.58
Chlorine	6.07
Potassium	0.71
Calcium	0.25
Barium	6.43

Rapid cooling rates in electron Beam Welding extend solid solubility which prevents segregation to a large extent and formation of a large eutectic. Solidification results in accumulation of elements Nb, Ti and Mo at the front of liquid/solid interface also may result in segregation to interdendritic area where carbide and Laves phase may form. The faster cooling rates prevalent in Electron Beam Welding suppress formation of the gamma at NbC eutectic. As shown in **Fig. 6** morphologies of inter-dendritic Nb-rich Laves phase may also form interconnected network [5].

**3.3 The examination of various phases formed in Electron Beam Welded Specimens**

In Inconel 718 various phases are present with varied morphologies. It is well established that gamma double prime, gamma prime, delta and NbC carbides have disc shape, globular, needle-like and blocky morphologies, respectively [7]. Delta phase (Ni<sub>3</sub>Nb) was identified in the HAZ which is precipitated from gamma double prime phase.

Evidence for the presence of Laves phase has been found in the fusion zone of alloy 718 weldments. It has been identified by its characteristic appearance, both in case of specimens welded in solution treated condition (as received) and those welded in aged condition (as received). Presence of this undesirable phase on solidification (i.e. Nb rich regions) accounts for lower ductility and impact strength of weldments. Extent of formation of this phase is dependent on the quantity of heat input, higher amounts of heat input will give slower cooling rates with consequent higher segregation, therefore more laves phase would be expected to form. This phase is dissolved by giving a post weld heat treatment i.e. solution treatment at 2000 F for 1 hour both in case of welds made in aged and solution treated condition. This is corroborated through the examination of microstructures (**Fig. 13 and 14**).

**3.4 Effect of Weld Heat**

Electron Beam Welding gives reduced thermal strain (which is almost 1/10th compared to other conventional welding processes) together with narrow fusion zone and HAZ, leads to two main metallurgical advantages,

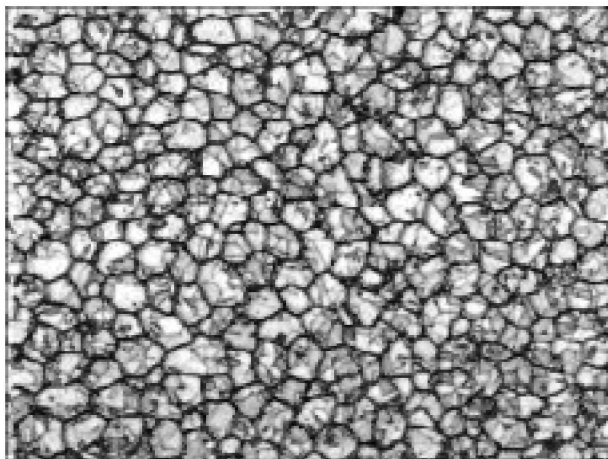
1. Reduced incidence of cracking during & after welding
2. Improved weld properties as there is reduction in metallurgical damage

As stated by W. Chan [11], during the heat treatment before welding and also during welding, segregation of impurities at grain boundary can take place. Segregation of sulphur on grain

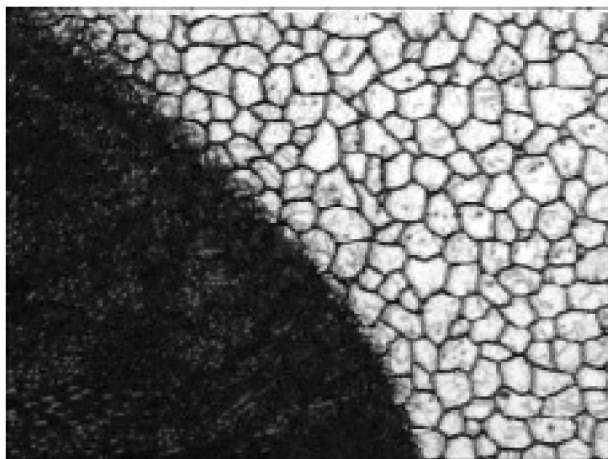
boundary can cause HAZ liquation cracking. If heating and cooling rates are rapid, it may not be possible for the impurities to travel to the grain boundaries [11]. In case of Electron Beam welding due to higher cooling rates, segregation of impurities at grain boundary is not observed as revealed through examination of microstructure.

**3.4 Effect of thermal treatment on grain size and shape**

The grain size measurement was done using microscopy for all three aforesaid variants of the welded specimens for the base metal and HAZ.

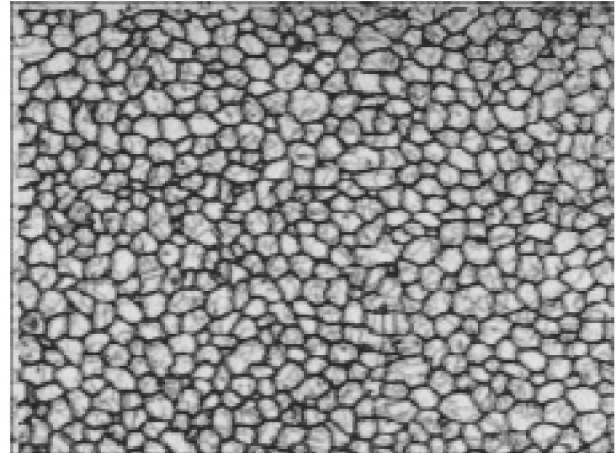


(i)

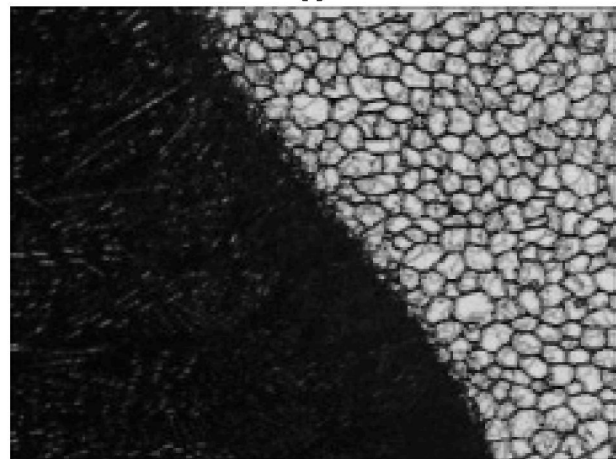


(ii)

**Fig. 17 : Grain morphology for specimen welded with plates (as received) in solution treated condition (i) Base Metal (ii) Heat Affected Zone, Magnification 100X, Etchant: Glyce-regia, ASTM grain size no 6-7**



(i)



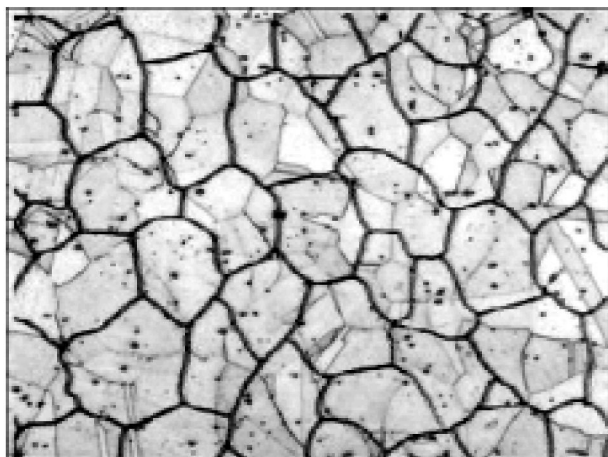
(ii)

**Fig. 18 : Grain morphology for specimen with plates as received in aged condition (i) Base Metal (ii) Heat Affected Zone Magnification 100X, Etchant: Glyce-regia, ASTM grain size no 7**

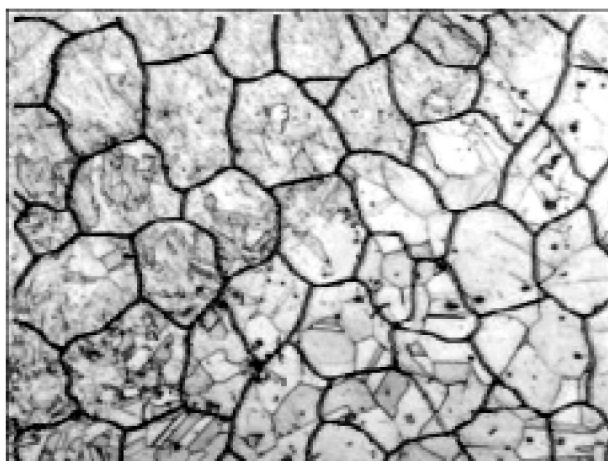
The heat affected zone have retained the fine grain structure (i.e. ASTM grain size of 6.5), of the parent metal thus successfully demonstrating the limited effect of heat during welding, for solution treated as well as aged samples. Also the morphology of grains remains the same for heat affected zone as that of base metal.

This result also justifies that the pre weld heat treatment did not show any remarkable change in the grain size.

**Fig. 18** shows significant grain coarsening due to Post weld heat treatment for base metal and HAZ. The results cannot be attributed to the welding process but is the outcome of Post weld Heat Treatment. Coarse grains are not conducive for high strength applications and should be avoided. This can be remedied through a suitable heat treatment to obtain a fine grained material.



(i)



(ii)

**Fig. 19 : Grain morphology for the specimen welded for plates in solution treated condition and administered PWHT (i) Base Metal (ii) Heat Affected Zone Magnification 100X, Etchant: Glyce-regia, ASTM grain size no 3-4**

### 3.5 Effect of thermal treatment on Mechanical Properties

Welding in the present context i.e of Inconel 718 by Electron Beam Welding establishes its efficacy over other methods of welding as confirmed in research carried by X. Cao et al.[3] where the parent metal was given solution treatment then welded and subsequently administered post weld aging treatment to achieve the desired strength.

**Table 7** [4][5] (Appendix-1) shows Comparison of tensile strength for specimens welded by EBW and LBW. The specimens in **Table 7** welded by EBW in aged condition (as received) had demonstratively achieved higher strength levels in comparison with specimen welded by LBW in aged condition.

Furthermore, the results of the mechanical properties for aforesaid three variants are tabled below, in **Table 8** (Appendix-2).

The main observation derived from the above evaluation tests explicitly demonstrated the Electron Beam Welded specimen in the solution treated condition, as received attained more than 100% joint efficiencies. Whereas the specimen welded in solution treated and aged condition the joint efficiency got reduced to 66.7%. This also resulted consequently in drop of UTS (0.2 proof stress) to 42.3% respectively welded in solution treated condition. The specimen administered solution treatment combined with double aging significantly resulted in increase in yield and tensile strength.

Furthermore the results of welds made on plates (as received in aged condition) demonstratively show the extent (i.e. small confinement), of heat affected zone on each side of weld which is approximately only 400 microns, The results of X Cao et al. [3] estimate similar HAZ extents of the order of 700 microns.

### 4.0 CONCLUSIONS

1. Microstructure examination reveals that the weld specimen are free of micro fissures, grain boundary segregation, solidification/ liquation / hot tearing cracks, and are free of lamellar tearing.
2. Microstructure examination of predominantly reveals the presence of gamma double prime/delta phase and Laves phase.
3. To obtain optimum level of mechanical properties in Electron Beam Welding, the welding should be preferably carried out for the material in solution treated condition and the weldment should be administered post weld solution and aging treatment.
4. Low levels of heat input obtainable with Electron Beam Welding in comparison with other methods of welding Inconel 718 do not alter the grain size of parent metal resulting in absence of degradation of mechanical properties.
5. Low levels of the heat input associated with Electron Beam Welding do not alter the grain morphology.
6. Microstructure in consistent with analysis in terms of various phases formed as a result of precipitation. It was observed that gamma double prime phase is present, which is major strengthening phase. Further Laves phase

was observed for plates in solution treated and aged condition, which was successfully dissolved after Post Weld Heat Treatment.

7. The microstructure examination for the different variants of welded samples clearly reveals absence of center line cracking.

## REFERENCES

1. ASM Metal Handbook (2000); Nickel and Nickel Alloys, Volume 2, 10th Edition, Properties and Selection: Nonferrous Alloys and Special-Purpose Materials, pp.1362-1404.
2. Sims TS, Stoloff N and Hagel WC (1987); Superalloy II: High Temperature Material for Aerospace and Industrial Power, John Wiley, New York.
3. Durand-Charre M (1997); The Microstructure of Superalloys, CRC Press, Amsterdam.
4. Lamba KBK (2008); Electron beam welding of nickel base alloy 718, Indian Welding Journal, 41(1), pp.34-43.
5. Cao X, Rivaux B, Jahazi M, Cuddy J and Birur A (2009); Effect of pre- and post-weld heat treatment on metallurgical and tensile properties of Inconel 718 alloy butt joints welded using 4 kW Nd:YAG laser, Journal of Materials Science, 44(17), pp.4557-4571.
6. Ping DH, Gu YE, Cui CY, Harada H (2007); Grain boundary segregation in a Ni-Fe-based (Alloy 718) superalloy, Material Science and Engineering A, 456(1-2), 99-102.
7. Chamanfar A, Sarrat L, Jahazi M, Asadi M, Weck A and Koul AK (2013); Microstructural characteristics of forged and heat treated Inconel-718 disks, Materials & Design, 52, pp.791-800.
8. Thompson RG, Dobbs JR, Mayo DE (1986); The Effect of Heat Treatment on Microfissuring in Alloy 718, Welding Journal, Welding Research Supplement, 65(11), pp.299s-304s.
9. Chaturvedi MC (2007); Liquation Cracking in Heat Affected Zone in Ni Superalloy Welds, Materials Science Forum, 546-549, pp. 1163-1170.
10. Lingenfelter A (1989); Welding of inconel alloy 718: a historical overview, Superalloy, 718, pp.673-683.
11. Chen W, Chaturvedi MC and Richards NL (2001); Effect of boron segregation at grain boundaries on heat affected zone cracking in wrought inconel 718, Metallurgical and

Materials Transactions A, 32(4), pp.931-939.

## BIBLIOGRAPHY

1. Vishwakarma KR, Richards NL and Chaturvedi MC (2005); HAZ microfissuring in EB welded ALLVAC 718 Plus alloy, Superalloys, 718, pp.625-706.
2. Knorovsky GA, Cieslak MJ, Headley TJ, Romig AD Jr and Hammett WE (1989); Inconel 718 a solidification diagram, Metallurgical Transactions A, 20(10), pp.2149-2158.
3. Ono Y, Yuri T, Nagashima N, Sumiyoshi H, Ogata T and Nagao N (2015); High-cycle fatigue properties of Alloy718 base metal and electron beam welded joint, Physics Procedia, 67, pp.1028-1035.
4. Chen W, Chaturvedi MC and Richards NL (2001); Effect of boron segregation at grain boundaries on heat- affected zone cracking in wrought inconel 718, Metallurgical and Materials Transactions A, 32(4), pp.931-939.
5. Hong JK, Park JH, Park NK, Eom IS, Kim MB and Kang CY (2008); Microstructures and mechanical properties of Inconel 718 welds by CO2 laser welding, Journal of materials processing technology, 201(1), pp.515-520.
6. Ono Y, Yuri T, Nagashima N, Sumiyoshi H, Ogata T and Nagao N (2015); High-cycle fatigue properties of Alloy 718 base metal and electron beam welded joint, Physics Procedia, 67, pp.1028-1035.
7. Henderson MB, Arrell D, Heobel M, Larsson R and Marchant G (2004); Nickel-based superalloy welding practices for industrial gas turbine applications, Science and Technology of Welding and Joining, 9(1), pp.13-21.
8. Gao P, Zhang K, Zhang B, Jiang S and Zhang B (2011); Microstructures and high temperature mechanical properties of electron beam welded Inconel 718 superalloy thick plate, Transactions of Nonferrous Metals Society of China, 21, pp.s315-s322.

## Acknowledgement:

The authors sincerely acknowledge the active support of the management of Parul University during the experimental investigations and of Dr. S.F. Xavier, Director R & D Parul University and Dr. G.S. Grewal, Deputy Director (Mechanical & Insulating Materials Division), Electrical Research and Development Association (ERDA) Vadodara for their valuable guidance.

**APPENDIX - I**

**Table 7 : Comparison of tensile strength for specimens welded by EBW and LBW [4][5]**

Pre/Post Weld Heat Treatment	Electron Beam Welding			Laser Beam Welding		
	Yield Strength, MPa	UTS, MPa	% Elongation	Yield Strength, MPa	UTS, MPa	% Elongation
Sted/As welded	448	880	58.2	451.9	897.2	39.6
STAed/As welded	983.61	1004	7.14	727.2	1031.1	2.9
STAed/STAed	1176.71	1317.27	7.14	1075.8	1318.2	16.5

**APPENDIX - II**

**Table 8 : Mechanical Properties for different variants of specimens welded by EBW [4]**

Pre/Post Weld Heat Treatment	UTS, MPa	0.2 Proof Stress, MPa	% Elongation	Joint Efficiency		Remarks
				% of UTS	% of 0.2 proof stress	
Sted/As welded	880	448	58.2	105.76	103.70	Fractured outside weld
Base Metal	832	432	60	-	-	-
STAed/As welded	1004.10	983.61	7.14	72	80.4	Broke in weld
Base Metal	1394.85	1223.18	31.8	-	-	-
STAed/STAed	1317.27	1176.71	7.14	113.72	124.96	Fractured outside weld
Base Metal	1158.33	941.67	30	-	-	-